Magnetohydrodynamic Continua and Stratification Induced Alfvén Eigenmodes in Coronal Magnetic Loops

A. J. C. Beliën, S. Poedts, and J. P. Goedbloed
FOM-Institute for Plasma Physics "Rijnhuizen," P.O. Box 1207, 3430 BE Nieuwegein, The Netherlands
(Received 25 September 1995)

The continuous spectra of a 2D inhomogeneous, cylindrical magnetic flux tube are studied and applied to solar coronal loops. The density is stratified radially as well as longitudinally, while other equilibrium quantities only vary in the radial direction. Stratification causes gaps to appear in the continuous spectrum, and it is shown that discrete global, stratification-induced Alfvén eigenmodes occur in these gaps. These global modes may be important for the heating of coronal loops.

PACS numbers: 96.60.Pb, 52.35.Bj, 95.30.Qd, 96.60.Ly

Continuous magnetohydrodynamic (MHD) spectra, global Alfvén eigenmodes in the gaps of these spectra, and damping of these modes have been the subject of intense research in fusion theory and experiments in the past few years (see, e.g., Refs. [1,2]). These modes occur due to a breaking of the poloidal symmetry in toroidal plasmas as compared to cylindrical ones, where the existence of continuous spectra is easily demonstrated. A similar breaking of symmetry occurs in solar coronal magnetic loops due to the longitudinal density stratification associated with the 10^9-fold increase of the density of the photosphere as compared to that of the corona. A corresponding study of the occurrence of gaps in the continua and global modes in these gaps for coronal loops has not been carried out so far. This is the subject of the present paper.

The equations of ideal magnetohydrodynamics possess two singularities that give rise to non-square-integrable solutions. In the spectrum of inhomogeneous MHD, these singularities are associated with continuous parts, the *Alfvén* and the *slow magnetosonic* continua. For the one-dimensional case, where equilibrium quantities depend on one spatial coordinate only, the relation between the singular positions and continuum frequencies can be written in algebraic form. For example, the Alfvén continuum is given by $\{k_\parallel(x)v_A(x)|x \in D\}$, where $k_\parallel$ is the component of the wave vector parallel to the equilibrium magnetic field, $v_A(x)$ is the Alfvén velocity, x is the spatial coordinate associated with the inhomogeneity, and $\mathcal{D}$ is the domain of x. However, these algebraic forms of the continua only apply to unbounded systems or bounded systems with periodic boundary conditions. In these two situations, the governing dynamic equation, the Hain-Lüst equation [3], is an ordinary second order differential equation in which the singularities are clearly visible. For 2D equilibria, algebraic descriptions for the continua simply do not exist due to the mathematical nature of the governing equations.

For more general longitudinal boundary conditions and 2D equilibria, singular behavior and field line resonances have been the subject of much research [4–12] and the results have found applications in fusion, magnetospheric, and coronal context. For a solar arcade model, the influence of a weak density stratification along the magnetic field lines was studied in Ref. [13]. Although the occurrence of gaps in the continuous spectra has been reported in this paper, the authors did not look for gap modes.

In this paper, we study the continua in a longitudinally stratified plasma cylinder as a model for a solar coronal loop and show that genuine 2D continua are present. The density stratification will couple distinct continua giving rise to annihilation of degeneracies and to continuum gaps. We will show that discrete global modes exist in these gaps.

We consider a cylindrical magnetic flux tube with length L and radius a, filled with hot plasma, and surrounded by a rigid wall. Curvature of the flux tube and gravity have been neglected. The two ends of the cylinder are in the photosphere, and the center is in the corona. The dynamics of the plasma column is studied within the framework of single fluid, ideal MHD, and for its description a cylindrical coordinate system (r, θ, z) is adopted. Since the ratio of thermal to magnetic pressure does not exceed 1% in the solar corona, the thermal pressure is neglected. The ideal MHD equations are linearized around a static force-free equilibrium, which is given by the dimensionless profiles

$$B_\theta(r) = \frac{\epsilon}{\alpha}\frac{d\psi}{dr}, \qquad B_z(r) = \sqrt{1 - 2\frac{\epsilon^2}{\alpha^2}A\psi\left(1 - \frac{1}{2}\psi\right)}, \tag{1}$$

in which $\epsilon \equiv 2\pi a/L$ is the inverse aspect ratio of the cylinder, and $\alpha \equiv 2\pi a^2 B_z(0)/\int_0^1 B_\theta(r)dr$ is a dimensionless quantity measuring the total azimuthal flux. The radial coordinate r is normalized to the plasma radius a and the magnetic field $\mathbf{B} = (0, B_\theta, B_z)$ is normalized to the value of the longitudinal component on axis, $B_z(0)$. The constant A and the function $\psi(r) \in [0, 1]$, which is a dimensionless azimuthal flux coordinate, are determined

from the force balance equation

$$\frac{d}{dr}\left(\frac{1}{2}B^2(r)\right) = -\frac{B_\theta^2(r)}{r}, \tag{2}$$

and $\psi(0) = 0, \psi(1) = 1$.

The equilibrium density profile can be chosen arbitrarily. We have chosen the following 2D profile:

$$\rho(r,z) = [1 - (1 - \rho_1)r^2] \times \left((\rho^p - 1)\exp\left[-\frac{\sin^2(\pi z/L)}{2\sigma^2}\right] + 1\right), \tag{3}$$

where $\rho_1\rho_p$ is the density at $r = 1$, $z = 0$, ρ^p is the value of the density at $r = 0$, $z = 0$, and σ is a density scale length. The profile is even with respect to $z = L/2$, and, for small values of the scale length σ, it represents a sharp transition from a high density region to a low density region.

The linearized ideal MHD equations are written in terms of the force operator equation

$$\mathbf{F}(\boldsymbol{\xi}) = \rho\,\frac{\partial^2\boldsymbol{\xi}}{\partial t^2}, \tag{4}$$

where $\boldsymbol{\xi}$ is the displacement vector and $\mathbf{F}$ is the well-known expression of the force operator [14]. Pressure effects have been neglected in $\mathbf{F}$. The following normal mode *ansatz* for the displacement field will be used:

$$\boldsymbol{\xi}(r,\theta,z,t) = (\xi_r(r,z), \xi_\theta(r,z), \xi_z(r,z))e^{\imath m\theta + \imath\omega t}, \tag{5}$$

with m an integer.

For a z-independent density profile and periodic boundary conditions the Alfvén continuum is given by the well-known algebraic description to which we referred earlier:

$$\Omega_{A,mn} = \left\{ \pm\omega_A(r) \;\middle|\; \omega_A(r) = \frac{mB_\theta(r)/r + n\epsilon B_z(r)}{\sqrt{\rho(r)}} \right\}, \tag{6}$$

where n represents the longitudinal Fourier mode number since, now, the z dependence can also be solved algebraically in terms of Fourier harmonics. In Fig. 1 several $m = -2$ continuum profiles are plotted. The continuum ranges themselves are found by projecting the different n branches onto the vertical axis. It is evident that the continua cover the entire axis, a property characteristic for 1D equilibria. Furthermore, the Alfvén modes (m,n) and (m,n') are degenerate at radial positions for which $(n - n')\epsilon rB_z(r) + 2mB_\theta(r) = 0$.

Because of the inhomogeneity of the magnetic field and the density, continuum eigenfunctions are localized at the resonant frequency where $\partial_r\xi_r \gg \xi_r$. This property can be used to reduce Eq. (4) to the following second order ordinary differential equation in z:

$$\left(\frac{\omega^2}{v_A^2(r_0,z)} - f^2(r_0)\right)\eta^0(r_0,z) = 0, \tag{7}$$

where $r_0 \in [0,1]$ is the radius of the singular layer, $v_A \equiv B/\sqrt{\rho}$ is the local Alfvén velocity, $\eta \equiv \mathbf{B}\times\boldsymbol{\xi}/B$ is the displacement component in the magnetic planes, perpendicular to the magnetic field, and $f \equiv (\mathbf{B}\cdot\boldsymbol{\nabla})/B$ is the gradient operator parallel to the magnetic field. The eigenfunctions of Eq. (7) represent the longitudinal behavior to zeroth order in the expansion around the singular layer.

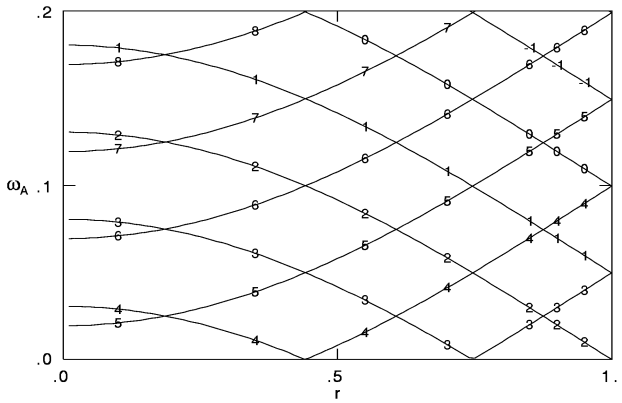

FIG. 1. Alfvén continua for an unstratified, periodic cylinder; for azimuthal mode number $m = -2$ and longitudinal mode numbers $n = -1, 0, 1, \ldots, 8$. Equilibrium parameters are $\epsilon = 0.05$, $\alpha = 1.254$, $A = 5.784$, $\rho_1 = 1$, and $\rho^p = 1$.

To numerically solve Eq. (7), both the equilibrium density and the displacement component η are approximated by a finite Fourier series,

$$\rho(r_0,z) = \sum_{n=-2N}^{2N} \rho_n(r_0)e^{\imath 2\pi nz/L}, \tag{8}$$

$$\eta^0(r_0,z) = \sum_{n=-N}^{N} \eta_n^0(r_0)e^{\imath 2\pi nz/L}. \tag{9}$$

From the $4N + 1$ density coefficients ρ_n only $2N + 1$ are independent. The other $2N$ are determined by the requirements that ρ is real and even. The coefficients η_n^0 are arranged in the vector

$$\boldsymbol{\eta} = (\eta_{-N}^0, \ldots, \eta_1^0, \eta_0^0, \eta_1^0, \ldots, \eta_N^0). \tag{10}$$

Using the orthogonality of the Fourier harmonics, the approximations (8) and (9) then turn Eq. (7) into the matrix operator form

$$\mathbf{R}\cdot\boldsymbol{\eta} = \omega^2\mathbf{D}\cdot\boldsymbol{\eta}, \tag{11}$$

with

$$R_{nl} \equiv \delta_{nl}\left(\frac{m}{r}B_\theta + \frac{2\pi}{L}nB_z\right)^2, \quad D_{nl} \equiv \rho_{n-l}. \tag{12}$$

Equation (11) implicitly carries the periodic boundary conditions that are imposed at $z = 0$ and $z = L$ because the individual Fourier modes already satisfy them.

The eigenvalue problem Eq. (11) is numerically solved using the QZ algorithm [15]. Figure 3 shows the results for an equilibrium with a strong density stratification (see Fig. 2), and with periodic boundary conditions. Compared with the unstratified density continua in Fig. 1, two striking differences are present.

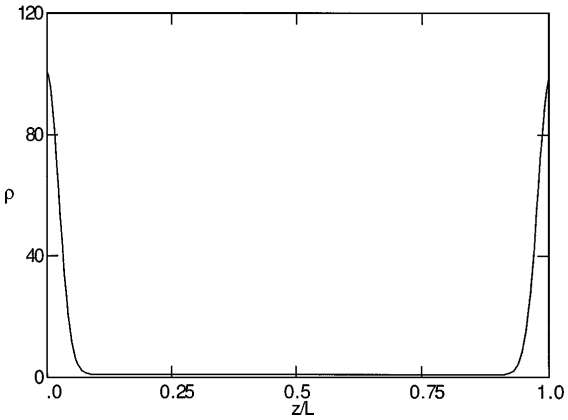

FIG. 2. Longitudinal stratification of the equilibrium density profile with $\rho_p = 100$ and $\sigma = 0.15$.

First, the degeneracies at the crossover positions are lifted. As a result, the projection onto the vertical axis shows gaps around the crossover frequencies (see the right-hand frame of Fig. 3). Furthermore, it is clear that different branches can be distinguished. However, they cannot be labeled with the longitudinal Fourier mode number since the longitudinal dependence is not described by single Fourier harmonics anymore. Investigating the Fourier decomposition of the longitudinal dependence of the continuum eigenfunctions reveals that the main harmonic contribution changes as the singular radius goes from 0 to 1. Changes take place around the crossover points as is indicated by the main mode contribution in Fig. 3 for the second branch from below.

Second, all frequencies are lower than in the corresponding unstratified case. The frequency decrease is a consequence of the increased mean density along the magnetic field lines. Hence, this is just an inertial effect.

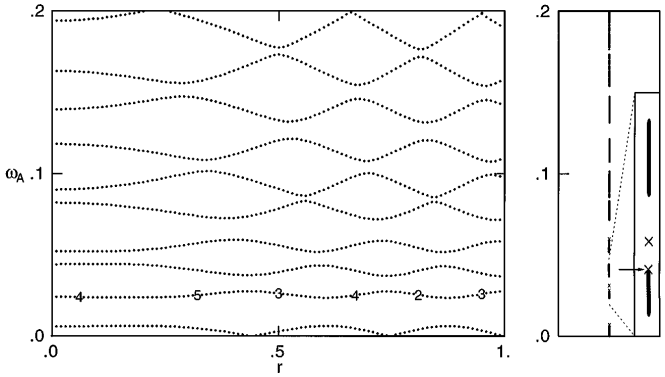

FIG. 3. The $m = -2$ Alfvén continuum of a 2D inhomogeneous, stratified, periodic loop for the longitudinal density stratification shown in Fig. 2. Number of Fourier modes: $N = 19$. Other parameters as in Fig. 1. The frame on the right shows the projection onto the ω axis, where crosses indicate the SAE modes. The inset shows an enlargement of the second gap.

To investigate the presence of global discrete MHD modes in the continuum gaps, the original Eqs. (4) have to be solved. This is done numerically with the finite element code POLLUX [16]. The results show that discrete modes exist in the continuum gaps. In Fig. 3 we have indicated the locations of these modes, which we will call *stratification induced Alfvén eigenmodes* (SAEs), by crosses for the lowest four gaps. In the first and fourth gaps from below one SAE is present, in the second gap two SAEs are present, but in the third gap no SAEs were found. Whether these modes are present, and how many, strongly depends on ρ^p and σ, which determine, in a complicated way, the coupling between the different Fourier coefficients. Since stronger coupling between the different Fourier modes that lift the degeneracies at the crossover points causes bigger gaps, the occurrence of SAEs is more likely in bigger gaps.

In Fig. 4 the mode structure of the gap mode in the second gap $[0.028\,28, 0.037\,53]$ closest to the edge of the continuum is shown: $\omega = 0.028\,45$. Since this mode is located close to the continuum edge, an accurate numerical convergence study was carried out to show that it is not a numerical error and that it is really located in the gap. The mode peaks at the two radii where the degeneracy has been lifted since mode coupling is strongest there. Notice that the longitudinal mode structure clearly shows a decrease in amplitude towards the ends of the loop indicating that this SAE will become a line-tied mode in the limit of an infinite density jump between the corona and the photosphere.

SAEs will continue to exist when nonideal MHD effects, such as resistivity, are taken into account. Their frequencies will be complex and the imaginary part, corresponding to the damping, will be proportional to the nonideal parameter involved. For resistivity, which is very small in the solar corona, this yields a very small damping. However, as shown in resistive MHD studies of gap modes in tokamak geometries [17], gap modes exist with a strong damping that converges to a constant value in the limit of zero resistivity. The strong damping is caused by the interaction with other continuum branches. It is to be expected that this also holds for SAEs in coronal loops. Strongly damped modes with a damping independent of resistivity and with a global mode structure can be excited easily and convert their energy quickly into heat and, therefore, play an important role in wave heating theories of the solar corona [16,18]. Resistive studies of SAEs and their heating properties will be addressed in a forthcoming paper.

Besides relevance for heating of coronal loops, global modes, such as the SAE modes, may play an important role in MHD spectroscopy of solar coronal loops, since they are in principle easier to observe than continuum modes. With a profound understanding of the relation between the physical parameters and the frequencies of global modes, valuable information on the magnetic field

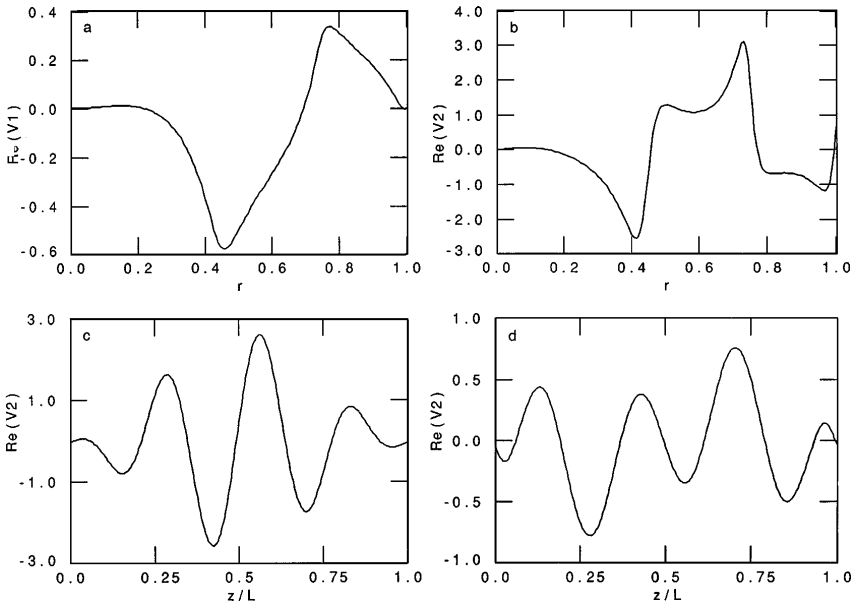

FIG. 4. Mode structure of the SAE mode in the second gap of the continuum, indicated by the arrow in Fig. 3, with $\omega = 0.028\,45$. The variables plotted are $v_1 \equiv r\omega\xi_r$ and $v_2 \equiv r\omega\eta$. (a), (b) Radial dependence at $z = 0.25$. (c), (d) Longitudinal dependence of v_2 at $r = 0.6$ and $r = 0.8$.

and density inside coronal loops can be obtained from their observed frequencies [19]. Gap modes may be observed by measuring the Doppler shifts of optically thin coronal lines originating from single coronal loops. This gives information on frequencies and mode structure of the waves involved. For this purpose, the Coronal Diagnostics Spectrometer aboard SOHO seems promising since its spatial and time resolution (1000 km and a few seconds) should be accurate enough to measure Alfvén periods of 100 s and longitudinal length scales of a few thousand to 10 000 km.

Summarizing, we have computed the Alfvén continua for a longitudinally stratified coronal loop. This stratification is responsible for gaps in the continuous spectrum. In these gaps global modes (SAEs) have been found which are a true consequence of the 2D nature introduced by the longitudinal density stratification. They may be important for wave heating of the solar corona and for solar MHD spectroscopy.

The authors wish to thank Hanno Holties and Ronald Nijboer for stimulating discussions and suggestions.

[1] R. Betti and J. P. Freidberg, Phys. Fluids B **4**, 1465 (1992).
[2] A. Turnbull, E. J. Strait, W. W. Heidbrink, M. S. Chu, H. H. Duong, J. M. Greene, L. L. Lao, and T. S. Taylor, Phys. Fluids B **5**, 2546 (1993).
[3] K. Hain and R. Lüst, Z. Naturforsch. **13A**, 936 (1958).
[4] J. P. Goedbloed, Phys. Fluids **18**, 1258 (1975).
[5] Y. P. Pao, Nucl. Fusion **15**, 631 (1975).
[6] A. L. Krylov, A. E. Lifschitz, and E. N. Fedorov, Dokl. Akad. Nauk. SSSR **247**, 1094 (1979).
[7] E. Hameiri, Phys. Fluids **24**, 562 (1981).
[8] A. L. Krylov and A. E. Lifschitz, Planet. Space Sci. **32**, 481 (1984).
[9] D. J. Southwood and M. G. Kivelson, J. Geophys. Res. **91**, 6871 (1986).
[10] M. Mond, E. Hameiri, and P. N. Hu, J. Geophys. Res. **95**, 89 (1990).
[11] G. Halberstadt and J. P. Goedbloed, Astron. Astrophys. **280**, 647 (1993).
[12] J. P. Goedbloed and G. Halberstadt, Astron. Astrophys. **286**, 275 (1994).
[13] S. Poedts and M. Goossens, Solar Phys. **133**, 281 (1991).
[14] I. B. Bernstein, E. A. Friedman, M. D. Kruskal, and R. M. Kulsrud, Proc. R. Soc. London A **244**, 17 (1958).
[15] C. B. Moler and G. W. Stewart, SIAM J. Numer. Anal. **18**, 241 (1973).
[16] G. Halberstadt and J. P. Goedbloed, Astron. Astrophys. **301**, 577 (1995).
[17] S. Poedts, W. Kerner, J. P. Goedbloed, B. Keegan, G. T. A. Huysmans, and E. Schwartz, Plasma Phys. Controlled Fusion **34**, 1397 (1992).
[18] S. Poedts and W. Kerner, Phys. Rev. Lett. **66**, 2871 (1991).
[19] J. P. Goedbloed, S. Poedts, G. T. A. Huysmans, G. Halberstadt, H. A. Holties, and A. J. C. Beliën, Future Generation Computer Systems **10**, 339 (1994).